EFFECTS OF ACOUSTIC LOADING ON THE SELF-OSCILLATIONS OF A SYNTHETIC MODEL OF THE VOCAL FOLDS

Li-Jen Chen
Department of Mechanical Engineering, McGill University, Montreal, Canada

Matías Zañartu
School of Electrical and Computer Engineering, Purdue University, West Lafayette, USA

Douglas Cook
Ray W. Herrick Laboratories, School of Mechanical Engineering, Purdue University, West Lafayette, USA

Luc Mongeau
Department of Mechanical Engineering, McGill University, Montreal, Canada

ABSTRACT

Synthetic models were used as test beds for the verification of mathematical models of voice production. A silicone synthetic model of the human vocal folds was used to investigate the influence of the acoustic properties of the subglottal and supraglottal tracts on the self-oscillation onset pressure and frequencies. The geometry and mechanical properties of the homogeneous synthetic model were selected based on available data.

The effect of acoustic loading on synthetic model was found to be significant. The lumped mass and sound propagation models developed by Zañartu et al. (2007) were used to verify the trends observed in the mechanical model. A wave reflection analog model was used for the acoustics of the subglottal and supraglottal tract (Zañartu, 2006; Story et al., 1997). The material properties and the system geometry were selected to match as closely as possible the experimental setup.

Satisfactory agreement between experimental and numerical results was found. The results confirm that the supraglottal tract is favorable to phonation, whereas the subglottal tract hampers the net energy transfer to the vocal folds oscillation, counterbalancing the effects of the vocal tract.

1. INTRODUCTION

Voiced sounds are produced by the flow-induced self-oscillations of the vocal folds. The vocal tract, as a resonator, plays a key role in the maintenance of these oscillations. Mathematical and synthetic models have been used to investigate the influence of the vocal tract on self-oscillation properties, since the usage of the larynx was limited by the degradation after dissection from the body. Austin and Titze (1997) found that the subglottal vocal tract had an influence on the amplitude of vocal folds vibrations in excised canine larynges with a pseudosubglottal system. Chan and Titze (2006) investigated the influence of acoustic loading on the phonation threshold pressure using a modified one-mass mathematical model (Titze, 1988). The inertive reactance of the supraglottal system appears in the onset pressure prediction formula. They found that the presence of an acoustic load tends to reduce the threshold pressure. Zhang et al (2006a; b) studied the influence of subglottal acoustic waves on the self-oscillations of laboratory models. The subglottal acoustic loading was systematically varied by changing the length of the subglottal tract. The dependence of vibration patterns on subglottal tract length suggested strong flow-acoustic interactions. The oscillatory modes of the physical model were described (Zhang et al., 2006b). The results suggested that the physical model primarily behaves like a single-mass model when acoustic loading is applied. Fluid-structure interaction (FSI) became more significant when a vertical constraint was imposed. Acoustically-driven phonation, where a strong source-resonator interaction is involved, has distinct characteristics from aerodynamically-driven phonation. In particular, a frequency lock-on with the subglottal resonance frequencies may occur. To eliminate strong fluid-sound interaction, caution must be exercised to keep subglottal formant frequencies away from the phonation frequency.

Although recent progress allows the inclusion of acoustic loading in continuum models of phonation (e.g., Alipour et al., 2000), such problem is modeled more efficiently using reduced order lumped mass models along with distributed sound propagation models (e.g., Story and Titze, 1995, and Zañartu et al., 2007). Zañartu et al (2007) showed that the subglottal acoustic loading may counterbalance the effects of the supraglottal acoustic loading using a

single-mass model. Significant fluid-sound interactions may dominate fluid-structure interactions in the maintenance of self-sustained oscillations.

To date, the influence of subglottal and supraglottal tracts acoustics on vocal folds vibrations has been investigated separately. No comprehensive empirical studies of the influence of the existence of both tracts have been conducted. In the present study, a physical model was used to study the respective influence of both subglottal and supraglottal tracts on vocal folds dynamics. Experimental observations were compared to predictions from the effective single degree of freedom model from Zañartu et al. (2007). The model parameters were adjusted to mimic the geometric, acoustics and physical considerations of the experimental setup. A method to obtain appropriate lumped mass parameters from a continuum model was also developed. The present study shows the contrary effects of subglottal and supraglottal tracts on onset pressures of the self-oscillations of the vocal folds.

2. MATERIALS AND METHODS

2.1 Model fabrication procedures

A schematic of the synthetic model is shown in Figure 1. The model geometry was based on the rigid model described by Scherer *et al*. (2001). The model was uniform along the anterior-posterior direction, with a length of 17 mm, and a slightly convergent glottal angle of $\theta = 5^{o}$.

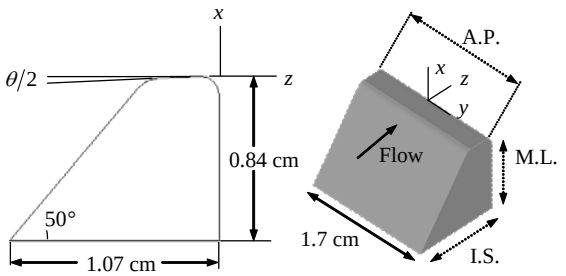

Figure 1: *Dimensions of the Synthetic Model. A.P.: Anterior-Posterior; M.L.: Medial-Lateral; I.S.: Inferior-Superior.*

Ecoflex 0030, a two-part platinum-catalyzed silicone solution, was used. The two parts (Part A and Part B) of the silicone solution were mixed in equal quantity. Silicone thinner was added to enhance the workability of the viscous silicone solution and the compliance of the silicone rubber after curing. Self-oscillations were obtained for reasonable subglottal pressure (1.6-2.0 kPa in current study). A ratio of Part A: Part B: Silicone Thinner of 1:1:3 was used. The construction details of the vocal folds model can be found in Thomson *et al*. (2005).

2.2 Experimental apparatus and method

Figure 2 shows a schematic of the experimental setup and configurations. The model folds were attached to acrylic mounts using silicone glue, over the anterior, posterior and lateral surfaces. The mounts were attached at the end of a rectangular transparent acrylic duct with a cross sectional area of $5\,cm^2$.

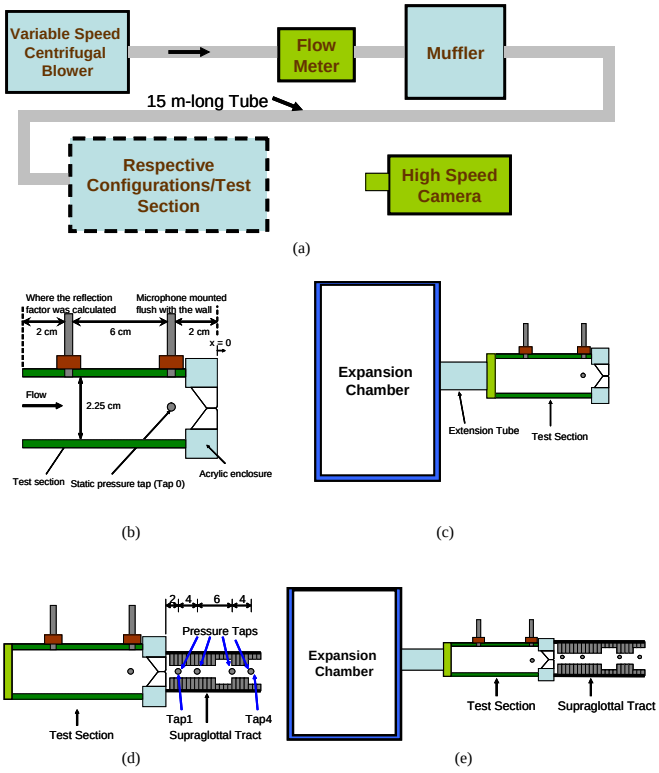

Figure 2: *Schematic and Configurations of the Setup: (a) Schematic of the Setup; (b) Configuration 1; (c) Configuration 2; (d) Configuration 3; (e) Configuration 4.*

Four different configurations were used. The baseline configuration, configuration 1 in Figure 2(b), had no supraglottal tract and a long tube with constant cross-sectional area, an anechoic subglottal termination. Two microphones and a static pressure tap were mounted flush within the side and top walls of the duct (at x = -2 and -8 cm, respectively).

In configuration 2 (Figure 2(c)), only the subglottal tract was attached and only the supraglottal tract was attached in configuration 3 (Figure 2(d)). Configuration 4 (Figure 2(e)) had both subglottal and supraglottal tracts. An

expansion chamber with inner volume of 6 liters was used to simulate human lung. A 10-cm-long PVC tube with a cross sectional area of $5\,cm^2$ was attached between the expansion chamber and the test section. The length of the subglottal tract was 20 cm. For supraglottal tracts, three different tracts, each with a length of 18 cm, were used. Tract 1 (T1) was a rectangular tube of constant area ($9\,cm^2$), while tract 2 (T2) and tract 3 (T3) were fabricated according to the MRI data of vowel /i/ and /a/ (Story et al., 1996) respectively. Four pressure taps were placed along the supraglottal tract, as shown in Figure 2(d). The distance between each tap was marked in the figure with the unit of cm.

The air was supplied by a centrifugal compressor with variable speed. A cylindrical plenum, 36 cm in diameter and 48 cm in height with a 2.54-cm-thick layer of fiberglass lining, was used to reduce noise inside the tube. The test section was connected to the cylindrical plenum using a flexible circular hose with an inner diameter of 2.54 cm, and a length of 15 m. The tube had the same cross section area as the test section. Air flow rate was measured using a general purpose mass-flow meter. The motion of the vocal folds model was captured using a high speed camera.

Table 1 shows the nomenclature for all tests. Throughout the present study, the upstream static pressure, or subglottal static pressure, always refers to the static pressure measured at the pressure tap closest to the vocal fold model (x = -2 cm), and the phonation frequency was always obtained from the microphone closest to the vocal model ($x = -2$ cm), as shown Figure 2(c). The subglottal and supraglottal static pressure, flow rate, and phonation frequency were recorded. The pressure drop across the vocal folds model was estimated from the static pressures measured at Tap 0 and Tap1, as shown in Figure 2.

Experimental Cases	Nomenclature
Config. 1	AcsCon1
Config. 2	AcsCon2
Config. 3 – Tract 1	AcsCon3T1
Config. 3 – Tract 2	AcsCon3T2
Config. 3 – Tract 3	AcsCon3T3
Config. 4 – Tract 1	AcsCon4T1
Config. 4 – Tract 2	AcsCon4T2
Config. 4 – Tract 3	AcsCon4T3

Table 1: Nomenclature for experiments

2.3 Numerical simulation

A lumped mass model was used to represent the synthetic model. The mass and spring stiffness values were derived from a continuum numerical analysis of the synthetic model. The viscous damping coefficient was measured experimentally. The geometry and material properties of the synthetic model were used to create a finite element model of the synthetic model. The material was found to have a density of 753 kg/m3 and a small deformation Young's modulus of 8.7 kPa. The numerical model consisted of approximately 13000 quadratic elements for a total of 25000 degrees of freedom. Refinement of this mesh resulted in less than 2% change in modal frequencies. Linear modal analysis was performed to obtain the first six modes of vibration. Because the fourth mode (135 Hz) most closely matched the fluid-induced vibration patterns of the physical model, this mode was used to establish the values of the lumped parameters. The extreme positions of the fourth mode are shown in Figure 3.

The lumped mass value was obtained by integrating the density over the volume of the numerical model, including a weight factor that was based upon the displacement at each point. The displacement field of the fourth mode shape was normalized by the maximum displacement, thus producing a displacement field ranging from zero to unity. This method effectively excludes all mass at the boundaries (zero displacement), and the remaining mass is included in the integral based on its displacement relative to the maximum displacement. Once the lumped mass value was obtained, the spring stiffness value was obtained by equating the natural frequency of the lumped spring-mass system with the modal frequency (135 Hz). Using the method outlined above, the following lumped mass parameters were obtained: m = 0.217 grams, k = 158.6 N/m. Note that the modal frequency is greater than the oscillation frequency observed in the experiments. More work is needed to correlate the modal analysis with experimental observations of the physical model.

The geometry of vocal tracts for the lumped mass model was available directly from the experimental setup. The sampling frequency (fs) was set to 44.1 kHz. The glottal opening shape was sinusoidal instead of rectangular to better account for the effect of the constraints at both anterior and posterior ends.

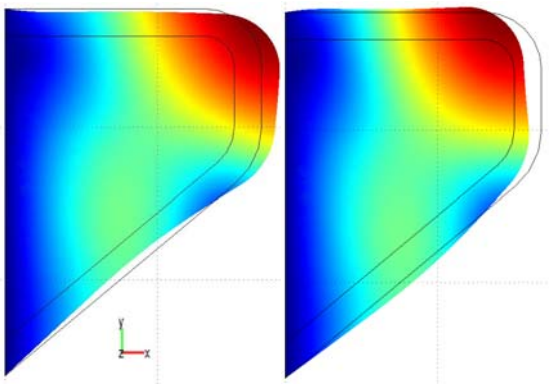

Figure 3: Transverse Displacement Extrema of the Fourth Mode (135 Hz)

Case	Subglottal Pressure (kPa)	Pressure Drop across VF (Pa)	Onset Flow Rate (L/Min)	Onset Frequency (Hz)
AcsCon1	2.06	2.06	61.97	107.5
AcsCon2	N/A	N/A	N/A	N/A
AcsCon3T1	1.76	1.83	46.76	107
AcsCon3T2	1.60	1.06	13.84	113.5
AcsCon3T3	1.61	1.23	16.76	120
AcsCon4T1	N/A	N/A	N/A	N/A
AcsCon4T2	1.97	1.26	21.96	339
AcsCon4T3	1.89	1.43	24.28	120.5

Table 2: Onset pressures for all cases

3. RESULTS AND DISCUSSION

3.1 Experimental results

Table 2 shows the subglottal static pressure, pressure drop across the vocal folds model, onset flow rate, and the onset fundamental frequency for all cases. For the reference case, AcsCon1, self-oscillations of the vocal folds model was achieved at a subglottal pressure slightly greater than those required by live larynges (0.6 – 1.6 kPa in loud voice) (Holmberg et al., 1988). Since no supraglottal tract was attached in AcsCon1, the pressure drop across the vocal fold models equaled the subglottal static pressure. Phonation frequencies, determined from power spectrum of microphone response, were close to that of a male human subject (Holmberg et al., 1988). Comparing AcsCon3T2 with AcsCon4T2, one can find the amplitude of the third harmonic component at 339 Hz increased in the power spectrum of the acoustic pressure. This is because the oscillation frequency was close to the resonance frequency of the subglottal tract (347 Hz). Phonation frequencies were influenced by resonance frequencies of vocal tracts.

The influence of supraglottal tracts on phonation properties was investigated in cases AcsCon3T1-3. Both the onset pressure and the onset flow rate were lower than those for the reference case. The supraglottal tract was found to facilitate the onset of vocal folds oscillation, which is consistent with previous findings (Titze and Story, 1997; Chan and Titze, 2006; Zañartu et al., 2007). The pressure drop across the vocal folds model for cases with the supraglottal tract was found to be lower than that of the reference case. This is because the supraglottal pressure is greater for cases with the supraglottal tract. The supraglottal pressure increases with the inertance of the supraglottal tract (Chan and Titze, 2006). Therefore, the pressure drop for T1 was much greater than that for T2 and T3 since the inertance for T1 was much smaller than that for T2 and T3.

No self-oscillation was achieved for AcsCon2 and AcsCon4T1, for flow rate up to the maximum capacity of the blower (flow rate = 80 L/Min). The subglottal tract increased the onset pressure and onset flow rate, as observed for AcsCon3T2-3 and AcsCon4T2-3. The subglottal tract was found to impede the onset of self-oscillation of the vocal folds model. This finding is also in agreement with previous findings (Austin and Titze, 1997, Zañartu et al., 2007).

3.2 Numerical simulation results and discussion

Numerical simulations were performed for all the configurations presented in the experimental section. Each configuration was simulated repeatedly to obtain onset values, for subglottal pressures ranging from 500 Pa to 5000 Pa. The stability analysis of each simulation was performed using phase portraits, as shown in Figure 4. Selected parameters are presented in Tables 3. Self-sustained oscillations were achieved only forAcsCon3T2-3 and AcsCon4T2-3. Subglottal pressures required for the onset of these cases were lower than those of their counterparts in the experiments. Despite differences in the subglottal pressure, the onset flow rates are close to those measured in the experiments.

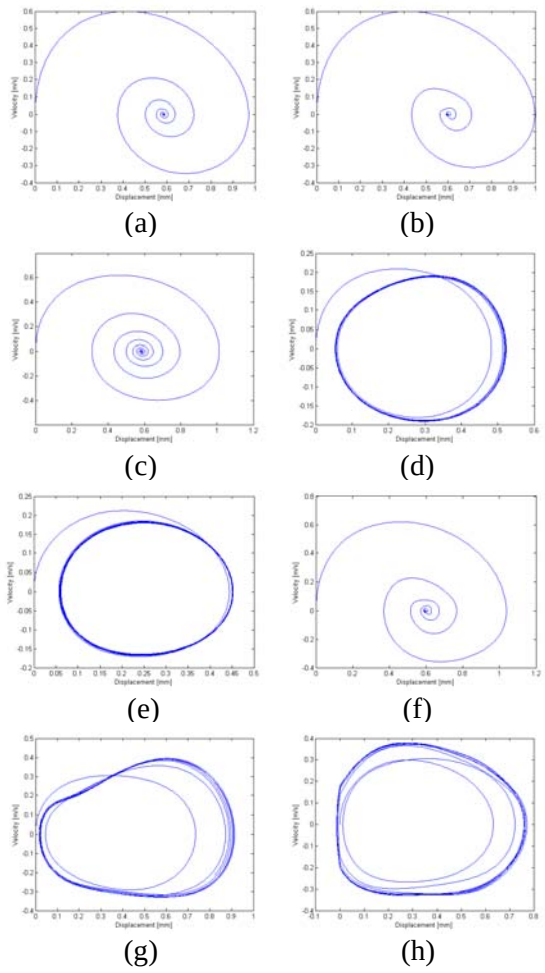

Figure 4: Phase Portraits of Cases in Numerical Simulation: (a) AcsCon1; (b) AcsCon2;(c) AcsCon3T1;(d) AcsCon3T2; (e)AcsCon3T3; (f)AcsCon4T1; (g) AcsCon4T2; (h) AcsCon4T3.

3.3 Discussion

The model was not able to maintain self-sustained oscillations unless a supraglottal tract with a narrow entry section was present. This behavior was expected for single-mass models since single-mass models can not oscillate in the absence of acoustic loading (Flanagan and Landgraf, 1968). This suggests that in AcsCon1 the physical model does not behave like a single oscillating mass.

Numerical simulations clarify the hampering effect of the subglottal tract with an expansion chamber. The results show that more inertive supraglottal loads (vowel /a/, in T3) facilitate phonation by reducing the onset pressure with respect to more compliant ones (vowel /i/, in T2).

The single degree of freedom theoretical model is not able to reproduce all the features observed in the experiments. This is likely due to limitations of the single-mass modeling approach. The main differences observed were reduced onset pressures, higher frequencies of oscillation, and reduced coupling with the third harmonic in AcsCon4T2.

Case	Subglottal Pressure (kPa)*	Onset Flow Rate (L/Min)	Onset Frequency (Hz)	Comment
AcsCon1	N/A	N/A	N/A	No onset
AcsCon2	N/A	N/A	N/A	No onset
AcsCon3T1	N/A	N/A	N/A	No onset
AcsCon3T2	0.88	13.88	135	
AcsCon3T3	0.87	14.41	141	
AcsCon4T1	N/A	N/A	N/A	No onset
AcsCon4T2	1.5	22.92	130	
AcsCon4T3	1.4	26.03	156	

** Lung pressures from 500 Pa to 5kPa*

Table 3. Results of numerical simulations for the single degree of freedom model

4. Conclusion

Supraglottal tracts facilitate phonation, whereas the subglottal tract hampers phonation. When strong acoustic coupling is present, a single-mass model may be sufficient to describe the basic physics of the self-oscillations. However, there are still discrepancies between the one-mass model and the physical model. A multi-degree of freedom model or the inclusion of an orifice discharge coefficient function in the single-degree of freedom model may be needed to improve the prediction.

5. REFERENCES

Alipour, F., Berry, D. A., and Titze, I. R., 2000, A finite-element model of vocal-fold vibration. J. Acoust. Soc. Am. 108(6): 3003–3012.

Austin, S. F., and Titze, I. R., 1997, The effect of subglottal resonance upon vocal fold vibration. Journal of Voice 11: 391-402.

Chan, R. W., and Titze, I. R., 2006, Dependence of phonation threshold pressure on vocal tract

acoustics and vocal fold tissue mechanics. The Journal of the Acoustical Society of America 119(4): 2351-2362.

Flanagan, J. L., and Landgraf, L. L., 1968, Self-oscillating source for vocal tract synthesizers. IEEE Trans. Audio Electroacoust, AU-16: 57–64.

Holmberg, E. B., Hillman, R. E., and Perkell, J. S., 1988, Glottal airflow and transglottal air pressure measurements for male and female speakers in soft, normal, and loud voice. The Journal of the Acoustical Society of America, 84(2): 511-529.

Scherer, R. C., Shinwari, D., Witt, K. J. D., Zhang, C., Kucinschi, B. R., and Afjeh, A. A., 2001, Intraglottal pressure profiles for a symmetric and oblique glottis with a divergence angle of 10 degrees. The Journal of the Acoustical Society of America 109(4): 1616-1630.

Story, B. H., and Titze, I. R., 1995, Voice simulation with a body-cover model of the vocal folds. J. Acoust. Soc. Am. 97(2): 1249–1260.

Story, B. H., Titze, I. R., and Hoffman, E. A., 1996, Vocal tract area functions from magnetic resonance imaging. The Journal of the Acoustical Society of America 100(1): 537-554.

Thompson, S. L., Mongeau, L., and Frankel, S. H., 2005, Aerodynamictransfer of energy to the vocal folds. J. Acoust. Soc. Am. 118(3): 1689–1700.

Titze, I. R., 1988, The physics of small-amplitude oscillation of the vocal folds. The Journal of the Acoustical Society of America 83(4): 1536-1552.

Titze, I. R., and Story, B. H., 1997, Acoustic interactions of the voice source with the lower vocal tract. The Journal of the Acoustical Society of America 101(4): 2234-2243.

Zañartu, M., Mongeau, L. and Wodicka, G. R., 2007, Influence of acoustic loading on an effective single mass model of the vocal folds. J. Acoust. *Soc. Am.*, **121**(2): 1119-1129.

Zhang, Z., Neubauer, J., and Berry, D. A., 2006a, The influence of subglottal acoustics on laboratory models of phonation. The Journal of the Acoustical Society of America 120(3): 1558-1569.

Zhang, Z., Neubauer, J., and Berry, D.A., 2006b, Aerodynamically and acoustically driven modes of vibration in a physical model of the vocal folds. J. Acoust. Soc. Am., 120(5): 2841-2849.